

# Proposed Search for a wind of Axion-like-particles using the Gravitational Wave Interferometers

Adrian Melissinos

*Department of Physics and Astronomy, University of Rochester  
Rochester, NY 14627-0171, USA*

10 March 2022

**Abstract**

## 1 Abstract

If ALPs exist they are expected to interact with the Electromagnetic field through a term of the form  $\mathcal{L}_{a\gamma\gamma} = -(g_{a\gamma\gamma}/4)F_{\mu\nu}\tilde{F}_{\mu\nu}\phi_a$ . Therefore if light traverses a region where an ALP field exists, its refractive index will be modified. We propose to measure the refractive index of light and its angular dependence as the Earth rotates with respect to the direction of the ALP wind, as evidence for the presence of such a wind. The LIGO interferometers are sensitive to differences in the refractive index of the light ( $\lambda = 1.064 \mu\text{m}$ ) circulating in the two arms, and such differences were recorded during the S5 run, February 2006 to July 2007 [1, 2]. They are due in part to the horizontal tidal gradients when they are aligned with one of the arms, imposing a shift on the frequency of the light circulating in that arm. In addition a very strong modulation was observed at twice the Earth's orbital frequency, as can be seen in Fig.1. This can be understood if the difference in refractive index between the two arms depends on the angle  $\theta$  between the light propagation vector  $\hat{k}$  and a "wind" of ALP's incident on the Earth from a fixed direction [3]. A difference  $\Delta(n_1 - n_2) \propto \sin^2(\theta_1) - \sin^2(\theta_2)$  reproduces the observed modulation. We present the data as a function of the Earth's motion, discuss the magnitude of the observed refractive index,  $\Delta n = n - 1 \approx 10^{-20}$ , and conclude that such data can reveal the angular dependence and magnitude of the refractive index of the light circulating in the arms in the presence of an ALP "wind".

## 2 Introduction

The LIGO interferometers are optimized for the detection of gravitational wave signals in the range 40-1000 Hz. However the difference in the phase of the light returning from the two arms to the detector (dark) port, that is the "signal", can also be recorded over long time intervals by using detection at the "free spectral range frequency" as explained in detail in [4]. The signal measured at the detector port is the difference in the phase shift of the light returning from the two arms

$$\Delta\phi = \delta\phi_1 - \delta\phi_2 \tag{1}$$

The individual phase shifts  $\delta\phi_j$ ,  $j= 1,2$  can in principle arise from changes  $\delta L_j$  in the effective path lengths  $L_j$  of the arms or a change in the frequency of the light. The net phase shift

can also be affected by modifications  $\delta\bar{n}_j$  in the effective refractive index  $\bar{n}$  experienced by the light propagating in the two arms. The net phase shift on the  $j_{th}$  arm for a single light traversal of length  $2L$  can be expressed as

$$\frac{\delta\phi_j^{(s)}}{2\pi} = \left( \frac{\delta L_j}{L} + \frac{\delta f_c}{f_c} + \frac{\delta\bar{n}_j}{\bar{n}} \right) \frac{2L}{\lambda} \quad (2)$$

In the operating mode, the interferometer is “locked” on a dark fringe by adjusting the carrier frequency  $f_c$  and the effective path lengths  $L_j$  using feedback so that  $\Delta\phi = 0$  is enforced at the detector port in the absence of a gravitational signal. Over a sufficiently large time interval  $T$  compared to the time between successive feedback actions the integrated net phase change reduces to an integral over changes in the difference

$$\Delta\bar{n}_{12} = \delta\bar{n}_1 - \delta\bar{n}_2 \quad (3)$$

of the effective refractive indices

$$\left\langle \frac{\Delta\phi}{2\pi} \right\rangle = \frac{1}{T} \int_{t-T/2}^{t+T/2} \frac{\delta\phi_j}{2\pi} \quad \text{or} \quad \frac{1}{T} \frac{2L}{\lambda} \int_{t-T/2}^{t+T/2} \frac{\Delta\bar{n}}{n} dt \quad (4)$$

because the changes  $\delta L_j$  and  $\delta f_c$  are stochastic and average to zero when the interferometer is locked.

The above demonstrate that the interferometer does have sensitivity to time varying signals arising from a difference in the index of refraction of the light circulating in each of the two orthogonal arms. The time variation of  $\bar{n}_j$  can be related to the Earth’s daily (siderial) rotation angular frequency,  $\omega_{\oplus} \approx 7.3 \times 10^{-5}$  rad/s, its annual orbital angular frequency  $\Omega_{\oplus} \approx 2 \times 10^{-7}$  rad/s, as well as to horizontal tidal gradients that “red shift” the frequency of the light circulating in the arms [4]. Such signals involve frequencies many orders of magnitude below the optimized band. At these low frequencies the instrumental noise prevents the extraction of the signal by the conventional detection process. However by taking advantage of information circulating in the interferometer at a sideband frequency, and of the long integration time that is available, the low and very low frequency signals can be extracted. This is discussed in detail in [5].

We consider data taken by the H1 (Hanford, WA) interferometer during the S5 LIGO run over a period of 16 months from April 2006 to July 2007. These data were reported in preliminary form in [1, 2] and consist of a time series of the amplitude of the signal at the dark port spaced at 64 second intervals. The signal amplitude is shown in Fig.1 for the entire 16 months of data taking. There are periods of time when no data is available because the interferometer was inoperative or had fallen out of lock. The signal amplitude is directly proportional to

$$\text{Amplitude} \propto \Delta n_{1,2} = \bar{n}_1 - \bar{n}_2, \quad (5)$$

namely the difference in the refractive index between the two arms.

Such a difference in refractive index can arise when a horizontal gravity gradient is present along one (but not the other) of the arms [5]. Indeed the tidal forces have a horizontal component along the arms, typically

$$g_{hor} \approx 10^{-7}g \approx 10^{-6} \text{ ms}^{-2} \quad (6)$$

which is time dependent as the Earth and the Moon rotate. The frequency and amplitude of these components is well known [6]. When the horizontal tidal gradient is aligned with one of the arms it imposes<sup>1</sup> a frequency shift (“red shift”) on the light circulating in the arm. The resulting phase shift with respect to the other arm, that is not aligned with the tidal gradient, is given for a single (round trip) traversal in the arm by

$$\delta\phi^{(s)} = 2 \int d\omega dt = 4\pi\nu_0 \int_0^L \frac{\delta\nu}{\nu} \frac{dx}{c} = \frac{4\pi}{\lambda_0} \int_0^L \frac{\Phi}{c^2} dx = \frac{2\pi}{\lambda_0} g_{hor} \frac{L^2}{c^2} \quad (7)$$

where  $\nu_0, \lambda_0$  refer to the carrier frequency,  $L$  is the length of the arm and  $\Phi = g_{hor}x$  is the gravitational potential. For  $g_{hor} = 10^{-6} \text{ m/s}^2$  the phase shift imposed on the LIGO interferometer for a single traversal is

$$\frac{\delta\phi^{(s)}}{2\pi} \approx 2 \times 10^{-10} \quad (8)$$

### 3 The time-dependence of $\Delta n_{1,2}$

To examine the time-dependence of the difference in refractive index between the two arms of the interferometer we spectrally (Fourier) analyze<sup>2</sup> the 14-month long time series shown in Fig.1. This reveals the presence of several discrete frequencies, centered around the Earth’s daily and twice daily rotation frequencies. The daily rotation frequencies are shown in Fig.2, and the twice daily in Fig.3. The frequency resolution is  $\Delta f = 1/(4T_{total}) = 6 \times 10^{-9} \text{ Hz}$  with<sup>3</sup>  $T_{total} = 4.2 \times 10^7 \text{ s}$ . The measured and known frequencies and amplitudes [6] are in excellent agreement as also shown in Table I, with two exceptions: in the daily group (see Fig.2) the dominant line is at  $f = 1.157 \times 10^{-5} \text{ Hz}$ , which corresponds to the exact daily (solar) rotation frequency, but the tidal line at this frequency, the S1 elliptic wave, has an amplitude that is 0.01 of the amplitude of the K1 declinational line<sup>4</sup>, at  $f = 1.606 \times 10^{-5} \text{ Hz}$ , namely it is completely unobservable. We conclude that the dominant line in the daily region is not understood and could be due to human activity, or thermal effects.

The twice daily frequencies are shown in Fig.3 and the four lines are all attributed to tidal gradients. They agree both in frequency (see Table I) as well as in magnitude with

---

<sup>1</sup>This is a manifestation of the direct coupling of the gravitational gradient to the light circulating in the interferometer.

<sup>2</sup>Because the data is not continuous we must use the Lomb-Scargle algorithm [7] which fits the data to a sine and cosine series.

<sup>3</sup>The factor of 4 is included because in the spectral analysis the data was oversampled by that factor.

<sup>4</sup>The K1 line is clearly resolved in Fig.2.

the known values [6]. The dominant line in this grouping is the Lunar principal wave M2 with an amplitude of 91  $\mu\text{gal}$ , (1 gal = 1 m/s<sup>2</sup>). We calculate the horizontal component of the tidal force along the arms of the interferometer at the latitude of the Hanford site, and for the orientation of the two arms. For the dominant M2 line we find

$$F_{South} \approx 0.7 \times 10^{-6} \text{ m/s}^2 \quad F_{West} \approx 10^{-6} \text{ m/s}^2$$

Thus the phase shift induced by the M2 line for a single traversal is

$$\Delta\phi^{(s)}/2\pi = 1.2 \times 10^{-10}$$

The measured power in the M2 line is obtained by integrating the spectral line in Fig.(3) over frequency<sup>5</sup>

$$\text{M2} \quad \text{Measured power 3538 counts} \quad \text{corresponds to} \quad \Delta\phi^{(s)}/2\pi = 1.2 \times 10^{-10} \quad (9)$$

Thus we can establish a relation between an observed power spectral density amplitude and the corresponding phase shift.

Table I. Observed and known frequencies of the tidal components (.Hz)

Symbol	Measured	Predicted	Origin, L=lunar; S=solar
<u>Long period</u>			
Ss <sub>a</sub>	$6.536 \times 10^{-8}$	$6.338 \times 10^{-8}$	S declinational
<u>Diurnal</u>			
O <sub>1</sub>	$1.07601 \times 10^{-5}$	$1.07585 \times 10^{-5}$	L principal lunar wave
P <sub>1</sub>	$1.15384 \times 10^{-5}$	$1.15424 \times 10^{-5}$	S solar principal wave
S <sub>1</sub>	$1.15741 \times 10^{-5}$	$1.15741 \times 10^{-5}$	S elliptic wave of <sup>s</sup> K <sub>1</sub>
<sup>m</sup> K <sub>1</sub> , <sup>s</sup> K <sub>1</sub>	$1.16216 \times 10^{-5}$	$1.16058 \times 10^{-5}$	L,S declinational waves
<u>Twice-daily</u>			
N <sub>2</sub>	$2.19240 \times 10^{-5}$	$2.19442 \times 10^{-5}$	L major elliptic wave of M <sub>2</sub>
M <sub>2</sub>	$2.23639 \times 10^{-5}$	$2.23643 \times 10^{-5}$	L principal wave
S <sub>2</sub>	$2.31482 \times 10^{-5}$	$2.31481 \times 10^{-5}$	S principal wave
<sup>m</sup> K <sub>2</sub> , <sup>s</sup> K <sub>2</sub>	$2.31957 \times 10^{-5}$	$2.32115 \times 10^{-5}$	L,S declinational waves

As can be seen by inspection of Fig.1, superimposed on the daily and twice daily oscillations is a modulation at much lower frequency. The spectral analysis reveals that this modulation is at twice the Earth's orbital frequency, within the frequency resolution as shown in Fig.4. The observed frequency is

$$f_{observed} = (6.239 \pm 0.6) \times 10^{-8} \text{ Hz} \quad \text{as compared to} \quad 2f_{\oplus\text{orbital}} = 6.338 \times 10^{-8} \text{ Hz} \quad (10)$$

<sup>5</sup>Since the true line width is narrower than the experimental resolution, the power is given by the area under the peak.

We attribute the observed time dependence of the difference in the refractive indices,  $\Delta n$  to the interaction of the light in the interferometer arms with a “wind” of ALPs that has a fixed direction in space. The wind arises because of the rotation of the spiral arm of the Galaxy that contains the Earth, through the static ALP background that permeates the Galaxy [8, 9]. We seek a dispersion relation that can reproduce the data. When light propagates through a cold ALP background, the refractive index is modified as shown by Espriou and Cerillo [10] but has no angular dependence.

Recently McDonald and Ventura have published a dispersion relation for light propagating through an ALP wind [11, 12]. Here  $(p_0, \vec{p})$  is the 4-vector of the ALP, and  $\theta$  the angle between the ALP momentum and the direction of the light,  $\hat{k}$ . Since the angle  $\theta$  changes continuously due to the Earth’s rotation with respect to the direction of the wind, we expect a corresponding change in the refractive indices along the two arms of the interferometer. The refractive index is given by Eq.(25) in [11],

$$\frac{|k| - \omega}{|k|} = -\delta n = -\frac{g_{a\gamma\gamma}^2}{16|k|^2} \left[ \dot{a}^2 + (\hat{k} \cdot \nabla a)^2 - 2|\nabla a|^2 \right] \quad (11)$$

$$\delta n = \frac{g_{a\gamma\gamma}^2}{16|k|^2} \left[ \omega_a^2 a_0^2 (1 + \beta_a^2 \cos^2(\theta)) - 2\beta_a^2 \right] \quad (12)$$

$$\delta n = \frac{g_{a\gamma\gamma}^2}{16|k|^2} 2\rho_a \left[ 1 - \beta_a^2 - \beta_a^2 (\sin^2(\theta)) \right] \quad (13)$$

In the above, the authors introduce the ALP-photon-photon coupling  $g_{a\gamma\gamma}$ , and state that the refractive index arises from the quadratic term in the dispersion relation; this is supported by referring to Fig.(2) of [12]. Further,  $a_0$  is the amplitude of the ALP field,  $\beta_a$  the ALP velocity and  $\omega_a \sim m_a$  the ALP energy, approximately equal to the ALP mass  $m_a$ ,  $a_0^2 m_a^2 = \rho_a$  is the ALP energy density which is well known from observational data to be  $\rho_a = 10^{-42} \text{ GeV}^4$  [13].

We have calculated the angles  $\theta_{1,2}$  of the two arms of the Hanford interferometer, properly oriented, and accounting for the Earth’s rotation, orbital motion and the motion of the solar system in the direction right ascension  $\alpha = 85^\circ$ , declination  $\delta = -29^\circ$  with a velocity in the SCCEF frame  $V_\odot = 500 \text{ km/sec}$ .

It follows from Eq.(13) that

$$\Delta_{n1,n2} = \frac{g_{a\gamma\gamma}^2}{16|k|^2} 2\rho_a [\sin^2(\theta_1) - \sin^2(\theta_2)] \quad (14)$$

Using the calculated angular dependence of the orientation of the interferometer arms, we have modeled Eq.(14). Spectral analysis of the modeled time series reveals a strong line at  $f = 2\Omega_\oplus$ , twice the Earth’s orbital rotation frequency, as observed in the data, confirming the angular dependence of the refractive index predicted by Eq.(14). An arbitrarily normalized fit of Eq.(14) to the data, as shown in Fig.(5), is satisfactory.

## 4 The magnitude of the refractive index.

From the power spectral density for the dominant line at the twice yearly orbital frequency, Fig.(4), and using the conversion factor of Eq.(9) we find that the phase shift  $\Delta\phi^{(s)}$  for light at  $\lambda \sim 1 \mu m$  propagating through the ALP wind incident on the Earth is of order

$$\Delta\phi^{(s)} = 8 \times 10^{-10\pm 1} \quad (15)$$

The refractive index is simply related to the phase shift

$$\Delta n = n - 1 = \frac{\lambda}{2L} \Delta\phi^{(s)}$$

and therefore we estimate that

$$\Delta n = n - 1 = 10^{-20\pm 1} \quad (16)$$

We expect the refractive index to depend on the ALP-photon-photon coupling, the ALP mass, the known ALP mass density, and the velocity of the ALP wind which we can take as  $\beta_a = 10^{-3}$ .

The magnitude of the angle dependent part is

$$\Delta n(\theta) = \frac{g_{a\gamma\gamma}^2}{16|k|^2} 2\rho_a \beta_a^2 \quad (17)$$

If we use the current upper limit [14]  $g_{a\gamma\gamma} < 10^{-10} \text{ GeV}^{-1}$ ,  $k = 1 \text{ eV}$ , and  $\rho_a = 10^{-42} \text{ GeV}^4$  and  $\beta_a = 10^{-3}$  we find  $\Delta n(\theta) = 10^{-51}$ , as compared to the measured value  $\Delta n(\theta) = 10^{-20}$ . Clearly Eq.(17) must be modified to describe the data. In the absence of theoretical guidance we use a dimensional argument and divide Eq.(17) by  $(m_a/\omega)^2$ ; in this case the observed refractive index can be recovered for

$$\frac{g_{a\gamma\gamma}/\text{GeV}^{-1}}{m_a/\text{eV}} = 3 \times 10^5 \quad (18)$$

which for  $g_{a\gamma\gamma} = 10^{-10} \text{ GeV}^{-1}$  [14] leads to  $m_a = 3 \times 10^{-16} \text{ eV}$ , which is not experimentally excluded but significantly different from the range predicted by the theoretical models [15].

We conclude that the gravitational Interferometers can be used to measure the refractive index of the light circulating in the arms to a precision of order

$$\Delta n = n - 1 \approx 10^{-20}$$

and its angular dependence. Such data can establish the presence of an ALP wind incident on the Earth, and the direction of the wind.

**Acknowledgments:** I am indebted to the LIGO team that made these measurements possible and in particular to D. Sigg, F.J. Raab, W.E. Butler, C. Forrest, T. Fricke and S. Giampanis who were involved in the the design, installation and operation of the fsr channel and in the analysis of the data. I also thank A. Kostelecky for insights on the effective refractive index in interferometers, and G. Ruoso and E. Milotti for constructive comments on a previous version of this note.

## References

- [1] A. Melissinos (for the LSC). The effect of the tides on the LIGO Interferometers, Twelfth Marcel Grossman Meeting on General Relativity, World Scientific, p.1718 (2012); arXiv:1001.0558
- [2] V.A. Kostelecky, A.C. Melissinos and M. Mewes, Phys. Lett. **B 761**, 1 (2016).
- [3] K. Freese arXiv:1209.3339
- [4] A. Melissinos “Observation of long term changes in the effective refractive index of light”, arXiv:1901.08442.
- [5] A. Melissinos “ On the Possible Detection of Low Frequency Periodic Signals in Gravitational Wave Interferometers”, arXiv:1410.0854.
- [6] P. Melchior, *The Tides of the Planet Earth*, Pergamon Press, 1978.
- [7] J. D. Scargle, ApJ 263, 835 (1982); W. Press, W. Vetterling, S. Teukolsky and B. Flannery, “Numerical Recipes in C++”, Cambridge University Press, 1988.
- [8] M. S. Turner, Phys. Rev. **D33**, 889 (1986).
- [9] The SAO Encyclopedia of Astronomy/Galaxy.
- [10] Espriou and Cerillo, arXiv:1512.03311v2.
- [11] J.I. McDonald and L.B. Ventura, arXiv:1911.10221.
- [12] J.I. McDonald and L.B. Ventura, arXiv:2008.1223.
- [13] See for instance A. Aoki and J. Soda, arXiv: 1608.05933
- [14] V. Anastassopoulos et al. Nature Physics, **13**, 584 (2017)
- [15] P.A. Zyla et al. (Particle Data Group), Prog. Theor. Exp. Phys. 2020, 083C01 (2020)

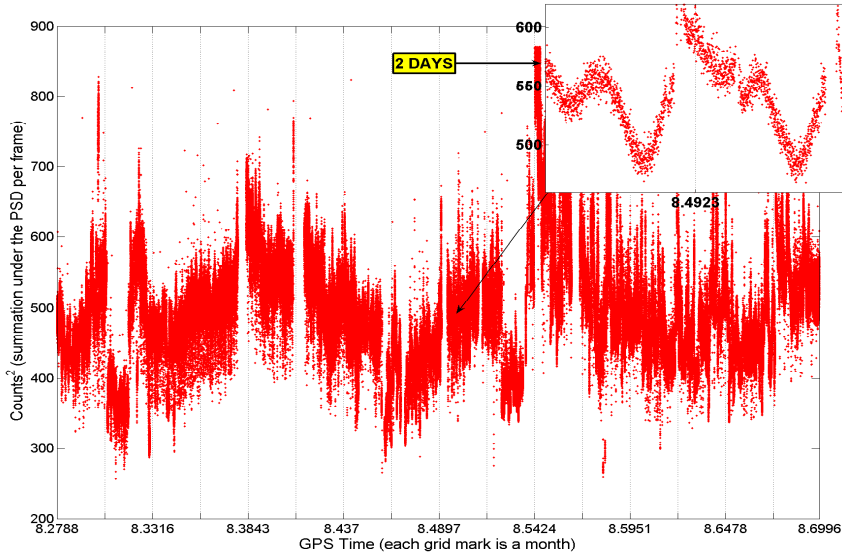


Figure 1: The integrated power spectral density in  $\pm 200$  Hz of the fsr as a function of time for 16 months during the S5 run. The daily and twice daily modulation can be seen in the inset. Vertical lines are at monthly intervals.

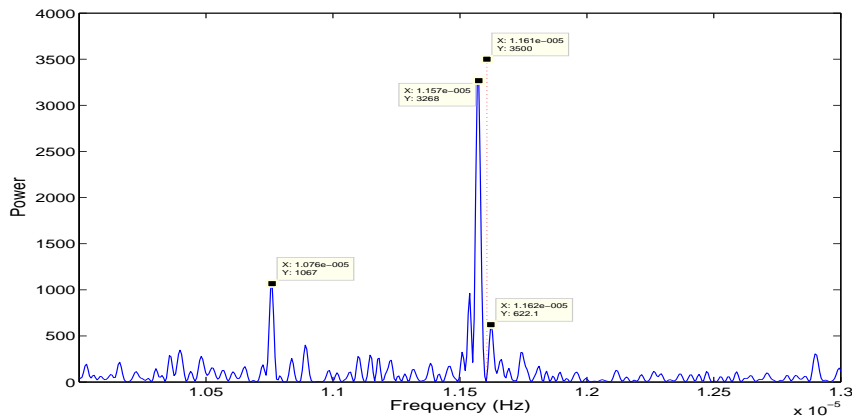


Figure 2: Power spectrum in the daily frequency region. The dominant line at a frequency  $f = 1.157e-5$  is at exactly at the daily solar rotation frequency, and is not understood at this time, but must be due to the interaction of the light in the arms with an external agent as the Earth rotates. The sidereal frequency is indicated by the dashed red line.



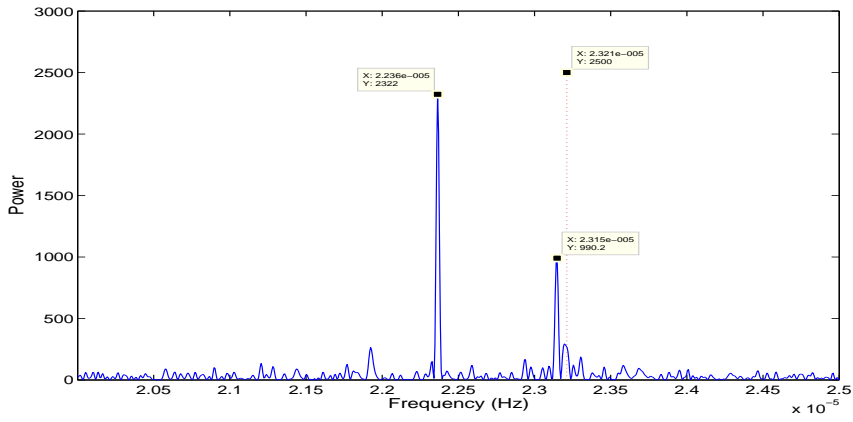


Figure 3: Power spectrum in the twice daily frequency region. All lines can be attributed to tidal gradients; see Table 1.

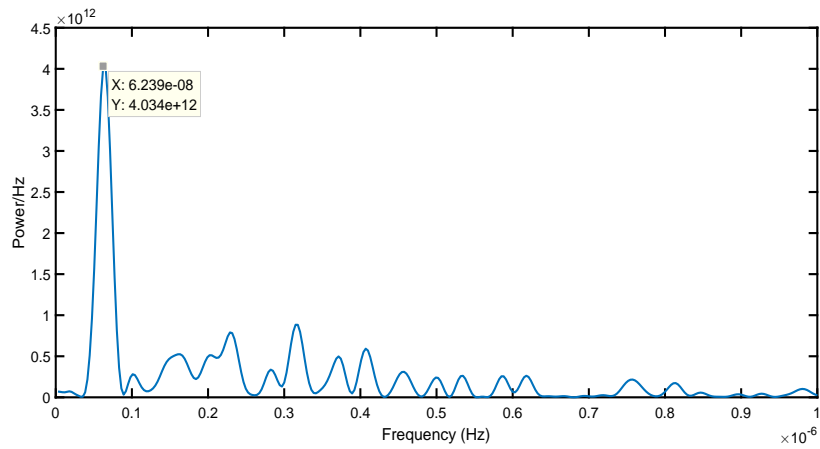


Figure 4: Power spectrum of the integrated power spectral density in the very low frequency region. The spectral line is at twice the Earth's yearly orbital frequency within the measurement error.

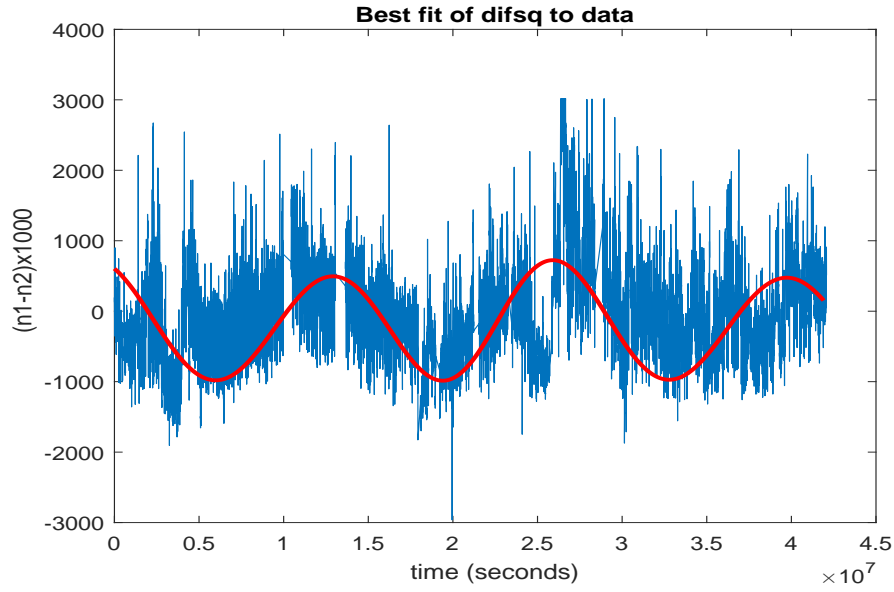


Figure 5: Fit of the predicted envelope of the daily oscillations (red)  $[\sin^2(\theta_1) - \sin^2(\theta_2)]$  to the data. Time in seconds starts at winter equinox of 2006. Normalization is arbitrary.